Chapter 5

Surface Morphology and Tribological Properties of Nanoscale (Ti, Al, Si, C)N Multilayer Coatings Deposited by Reactive Magnetron Sputtering

Mei Wang and Shojiro Miyake

Additional information is available at the end of the chapter

http://dx.doi.org/10.5772/intechopen.73141

Abstract

The current topics related to the morphology and tribology of TiAlN monolayer, TiAlN/SiNx, TiAlN/CNx and TiAlN/CNx±CNx nanoscale multilayer coatings and refer to our recent results on the evaluation of surface morphology, and nanoscale mechanical and tribological properties of coatings deposited on cemented carbide cutting tools and silicon wafer substrates by reactive magnetron sputtering deposition. The surface morphology and microstructure of the coatings were evaluated with an atomic force microscope in dynamic friction mode together with transmission electron microscope imaging. The tribological properties of the coatings were evaluated by pin-on-disc friction testing in dry air, and high-frequency linear-oscillation friction testing under various lubrication conditions. The tribological properties of the multilayer TiAlCrSiN and TiAlSiN coatings were compared with those of a single layer TiAlN coating to evaluate their possible applications to the surfaces of cutting tools. The machining performances of single layer TiAlN, multilayer TiAlSiN, and TiAlCrSiN coated drills were investigated in drilling of carbon steel.

Keywords: surface morphology, tribological property, nanoscale multilayer, atomic force microscope, cutting tools

1. Introduction

Currently, thin hard physical vapor deposition (PVD) coatings are widely used to improve the tribological performance of forming tools, cutting tools, and machine elements [1]. In these applications, the surface morphology and tribology of the coated part are the most important factors influencing the tool and equipment performance [2]. Cutting tools might be used in

harsh machining environments without lubrication or under water-lubricated conditions. Tribological applications of thin films to cutting tools have considerably extended tool life and enabled the realization of dry machining and high-speed machining of hardened materials [3, 4]. Films of diamond-like carbon (DLC) and transition-metal and carbon nitrides (CNx), such as titanium aluminum nitride (TiAlN) and CNx are the most widely used coatings for tribological applications, such as for forming and cutting tools. Thus, it is desirable to improve the tribological properties of these films to enhance their performance in tool applications [5].

In this chapter, topics related to evaluation of the surface morphology and tribological properties of thin films are reviewed. Our recent results on the morphology and tribological properties of TiAlN monolayer, and TiAlN/SiNx and TiAlN/CNx multilayer coatings deposited on cemented carbide cutting tools and silicon wafer substrates by reactive magnetron sputtering deposition are referred in [4, 6, 7]. First, nanoscale TiAlN/SiNx multilayer films were deposited to improve the hardness of TiAlN; we found that the mechanical properties of the multilayer film were considerably improved compared with those of the monolayer film [4]. The introduction of a SiNx layer led to the formation of hard coatings owing to suppression of the TiAlN grain growth, grain refinement, and a decrease in surface roughness. A decrease in the grain diameter and associated decrease in surface roughness likely led to improved mechanical and tribological properties of the coatings [4]. However, the wear performance of the TiAlN/SiNx coating under ambient or high-temperature conditions showed negligible improvement because of its high friction coefficient. Second, CNx is an important tribological material and CNx thin films feature attractive properties such as improved hardness and elasticity and a lower friction coefficient [8, 9]. CNx thin films are currently being extensively studied for their potential tribological applications owing to their favorable mechanical and tribological properties [10]. These materials have already found applications as protective overcoatings for hard discs and read/write heads [11, 12]; furthermore, such materials are of interest in the field of nanotechnology owing to their high wear resistance and low friction properties [11, 12]. It has been found that amorphous CNx films exhibit good wear resistance with a low coefficient of friction (COF) in the range of 0.07–0.3, which is dependent on the N/C ratio and the fraction of the sp3-bonded carbon in the film [8, 9]. Therefore, attention has been paid for combining low COF CNx and hard nitrides together by forming composites or multilayer coatings to achieve the desired mechanical and tribological properties, for example, TiN:CNx composite films [13, 14], and CNx:TiN multilayer coatings [15, 16].

Several studies have indicated that multilayer coatings can exhibit high hardness and fracture resistance with low compressive stress through control of the parameters of the layered structure [5, 17]. The tribological behavior of carbon-based thin films is also strongly influenced by their chemical composition, polycrystalline structure, and surface morphology [18]. However, there remain uncertainties regarding the effects of the deposition of (Ti,Al)N, TiAlN/SiNx, TiAlN/CNx, and CNx coatings on the surface morphology, microstructure, and tribological properties of these coatings. The potential for low friction coefficients and high resistance to abrasive wear are important characteristics for high-speed and hard material cutting applications. In investigations that have aimed to increase the wear resistance and tribological properties of TiAlSiN coatings for wet cutting applications, improved tribological properties have been achieved through the incorporation of chromium (5–10 at%) into PVD TiAlSiN coatings [19–22].

The wet (water soluble fluid) machining performance of single layer TiAlN, and multilayer TiAlSiN and TiAlCrSiN coatings were assessed when drilling into a carbon steel workpiece (S50C, 50-53HRC). The objective of the present study was to assess the performance of 6-mm diameter WC–Co drills (OSG Corporation, Japan). The critical wear regions of the drills were examined metallographically with the use of a scanning electron microscope (SEM) to identify wear mechanisms acting at the cutting edges of the single layer TiAlN and multilayer TiAlCrSiN coated drills.

This chapter is focused on the influence of morphology on the tribological properties of TiAlN, TiAlN/SiNx, and TiAlN/CNx multilayer coatings with and without a CNx top layer deposited on Si(100) and cemented carbide tool steel (WC) substrates. We also compare the performance of the multilayer coatings with that of a TiAlN monolayer with and without a CNx top layer. To study the friction behavior of these films, in relation to their various structures and surface morphologies resulting from the deposition parameters, we measured the microstructure and surface morphology of the films by transmission electron microscope (TEM) and SEM imaging together with atomic force microscope (AFM) measurements. Vickers hardness, pin-on-disc friction, and high-frequency linear-oscillation (SRV) friction testing were also used to study the tribological properties and wear resistance of such coatings. Furthermore, we compared the tribological properties of the multilayer TiAlCrSiN and TiAlSiN coatings with those of a single layer TiAlN coating to evaluate their possible application to surfaces of cutting tools. The machining performance of the single layer TiAlN, multilayer TiAlSiN, and TiAlCrSiN coated drills were investigated in the drilling of carbon steel (S50C, hardness 50HRC).

2. Experimental methods

2.1. Sample preparation

Figure 1 shows a schematic illustration of the multi-target DC reactive magnetron sputtering equipment used in this experiment. The equipment consisted of four independent target holders and DC power was applied to both the target holders and the substrate holder. As shown in **Figure 2**, in this study we prepared: a TiAlN monolayer (TiAlN), a TiAlN/SiNx multilayer, and a TiAlN monolayer with a CNx top layer (TiAlN+CNx), a TiAlN/CNx multilayer with a top TiAlN layer (TiAlN/CNx+TiAlN), and a TiAlN/CNx multilayer with a CNx top layer (TiAlN/CNx+CNx) [4, 6, 7]. All coatings were prepared on polished Si wafers and cemented carbide tools by DC magnetron sputtering from TiAl alloy (50/50 at%, 99.99% purity), carbon (99.99% purity), and Si (99.99% purity) targets. Alternating deposition of TiAlN and SiNx or CNx layers was applied to realize the TiAlN/SiNx and TiAlN/CNx multilayer coatings [4, 7]. Full details of the deposition process have been previously reported [7]. The coating process consisted of three steps such as heating, cleaning by ion bombardment, and multi-nanolayer coating. The system base pressure was maintained at approximately 3.5×10^{-3} Torr to produce enough Ar ions for ion bombardment cleaning of the substrate [4]; the substrate was heated at a power of 7000 W for 30 min prior to deposition and the substrate temperature was maintained at ~420°C for the deposition. During the ion bombardment

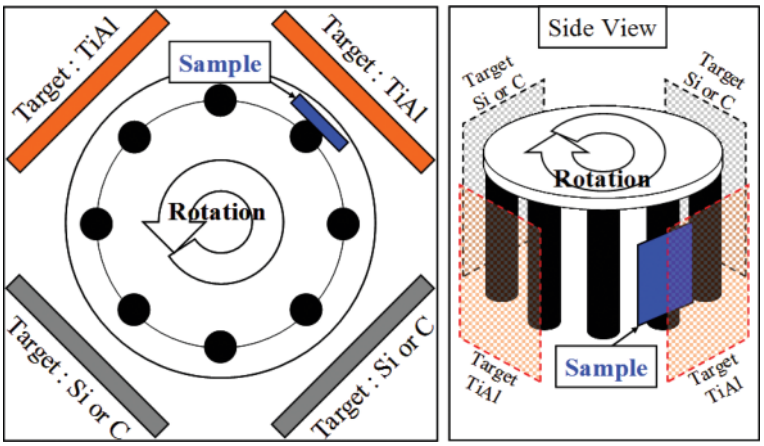

Figure 1. Schematic of DC sputtering equipment.

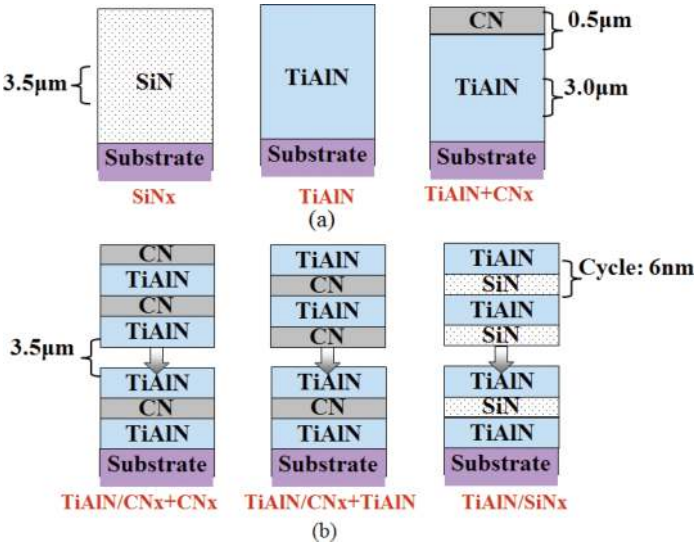

Figure 2. Samples of mono- and multilayer coatings.

cleaning process, Ar ions were directed at the substrate with a substrate bias of −500 V. Subsequently, the multi-component multi-nanolayer films were coated with a gas mixture of Ar (220 ml) and N_2 (160 ml). On the basis of preliminary experiments, the optimal deposition parameters were determined and multilayer coatings were fabricated. To compare the frictional properties of the monolayer and multilayer coatings, the total film thickness of the TiAlN, or TiAlN/CNx layers was set to be 3 μm. The CNx top layer was approximately 0.5 μm. For multilayer coatings, the layer period was set to be approximately 7 nm and the thickness of the TiAlN layer was approximately 6 nm [4, 7].

2.2. Morphology and microstructure observations

The microstructures of the coatings were evaluated by TEM and SEM cross-sectional imaging. AFM was used to observe the surface of the TiAlN, SiNx, TiAlN/SiNx, TiAlN+CNx, TiAlN/CNx+TiAlN, and TiAlN/CNx+CNx coatings [4, 7]. The morphological characteristics of the coatings were measured with the use of AFM in dynamic friction mode (DFM) with a carbon nanotube tip having a radius of approximately 44 nm. The AFM system (Digital Instruments Nanoscope III, Hysitron Inc.) was used. Calculations were performed within the scanning probe image processor (SPIP) software, which is a standard program for processing AFM data at the nanoscale. The grain diameter and surface roughness of the coatings were determined by scanning an area 3 × 3 μm with the AFM. To investigate the effects of grain diameter on the surface morphology and the boundaries between the grains, simulations were performed to calculate the mean grain diameter and surface roughness of the scanning area. The coating surfaces were characterized with the use of the roughness analysis module; the values for surface roughness, average roughness (calculated by Sa: distance between peaks), and peak-peak roughness (calculated by Sy: height difference between the highest and lowest peaks in the image), were obtained by analyzing the images and cross-sectional profiles and measuring the mean grain diameter parameters.

2.3. Mechanical and tribological properties evaluation

Mechanical properties, including hardness and adhesion strength were measured by Vickers hardness and scratch testing (CSM Instruments SA). The load used for hardness measurements was 0.025 N. A scratch tester was used to apply an increasing load with a spherical diamond indenter having a radius of approximately 0.2 mm. The critical load Lc, determined by acoustic emission (AE) observations of the scratch, was used as a quantitative measurement. Full details of the methods used in the hardness and scratch tests have been previously reported [4].

The tribological properties were evaluated from pin-on-disc friction and SRV testing methods. The pin-on-disc wear test was performed at an air humidity of 50 ± 10% and a temperature of

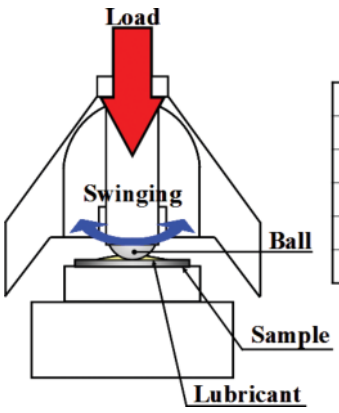

Tab.1 Friction test conditions

Load:	10N
Stroke:	500μm
Frequency:	50Hz
Number of Cycles:	30000times
Ball:	SUS440C 6.0mm
Lubricant:	Dry, Water, PAO

Water: Tap water
PAO : Poly Alpha Olefin

Figure 3. Swing type friction tester (SRV).

25 ± 3°C with the use of a pin-on-disc tribometer with a counterpart composed of SUS304 steel, placed horizontally on a turntable. The wear test was performed at a load of 0.5 N and a linear speed of 100 mm/s for a total sliding time of 600 s (corresponding to a sliding distance of 60 m). The frictional coefficients were calculated by measuring the frictional force from the wear scar area. In the SRV tests, the two test specimens, namely balls and discs, were installed in the test chamber and pressed together. As shown in **Figure 3**, the upper specimen was oscillated over the lower specimen at pre-programmed frequency, stroke, load, and temperature settings. In this study, the test was conducted with the use of an AISI440C ball indenter (SUS440C, 6.0 mm diameter) without lubricant under a 10 N load, with the use of a 500-μm stroke, a 50-Hz frequency, and 30,000 revolutions at room temperature and atmospheric pressure (30–45% humidity). The wear profiles of the coatings were measured by the SRV test.

3. Result and discussion

3.1. Microstructure and morphology

SEM micrographs of the film fracture cross-sections are shown in **Figure 4** for the TiAlN monolayer with a thickness of approximately 3 μm and the TiAlN/SiNx and TiAlN/CNx multilayer coatings with a total thickness of approximately 3.6 μm [7]. TiAlN has a columnar morphology, as shown in **Figure 4a**. The introduction of SiNx into the coating system changed the fracture morphology of TiAlN from a columnar microstructure to a fine-grained structure

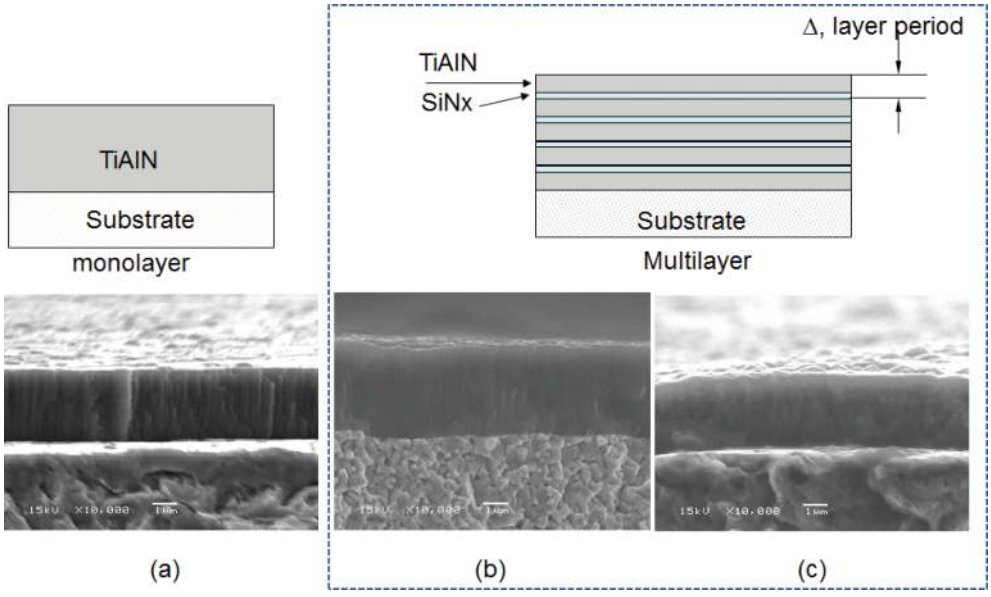

Figure 4. Cross-sectional image of TiAlN monolayer, and TiAlN/SiNx and TiAlN/CNx multilayer coatings.

http://dx.doi.org/10.5772/intechopen.73141

of TiAlN/SiNx, as shown in **Figure 4b**. This effect could be attributed to growth of the primary nuclei on the top layer (**Figure 4b**). This result indicates that growth of crystals was blocked periodically by the development of the surface covering layer, which covered the whole surface of the crystals and suppressed grain growth [4, 7, 23]. **Figure 4c** shows a SEM image of a fracture cross-section of a TiAlN/CNx coating. The TiAlN/CNx also showed a fine-grained structure owing to the introduction of CNx into the coating system [7].

Figure 5 shows TEM images of the microstructure of a TiAlN/SiNx multilayer film. The TiAlN/SiNx was formed by alternation of the TiAlN and SiNx layers at a rotation speed of 3 revolution per minute (rpm) [4]. A nanolayered structure composed of sequentially alternating TiAlN and SiNx layers was confirmed [4]. High resolution TEM images of the TiAlN/SiNx nanolayer cross-section exhibited a bilayer period of 6–8 nm and nanometer-sized grains. The white arrows in the figure indicate the film growth direction. The film morphology showed a dense columnar structure.

Figure 6 shows a TEM image of the microstructure of a TiAlN/CNx+CNx multilayer film. As shown in area I (**Figure 6a**, marked by an arrow), the bright dots indicate the presence of a CNx top layer phase with a uniform amorphous structure. In areas II and III of **Figure 6a** (indicated by arrows), micro-diffraction patterns featured both individual spots and continuous rings that corresponded to the superposition of individual diffraction patterns of TiAlN and CNx [7]. **Figure 6b** shows that the film morphology was fine-grained and that the growth directions of the TiAlN and CNx layers alternated, as indicated by the dark and bright layers, respectively. **Figure 6c** shows that the TiAlN nanolayers in the TiAlN/CNx coating were approximately 5-nm thick and separated by a matrix of amorphous carbon [4]. This result suggests that the TiAlN/CNx multilayer had a modulated structure with a periodicity of approximately 7 nm, indicating that the nanolayered structure was composed of sequentially alternating TiAlN/CNx, owing to the rotation speed of 3 rpm [4, 7, 23, 24].

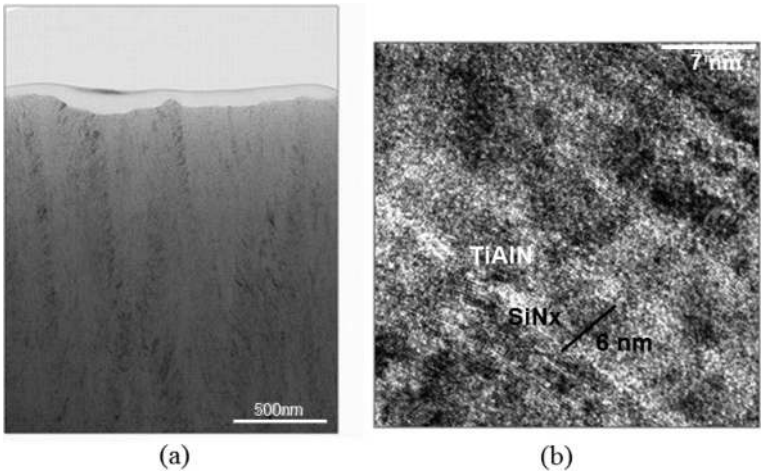

Figure 5. Cross-sectional TEM images of TiAlN/SiN coating, observed at scale of (a) 500 nm and (b) 7 nm.

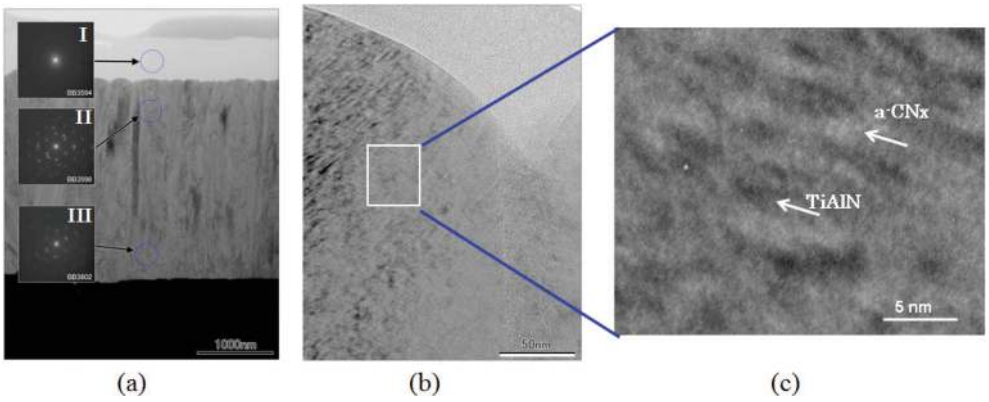

Figure 6. Cross-sectional TEM images of the TiAlN/CNx + CNx coating observed at scales of (a) 1000 nm, (b) 50 nm, and (c) 5 nm.

The surface morphology and roughness of the films were observed by AFM in DFM and analyzed by collecting three-dimensional surface profile data. The mean grain diameters of the samples were determined by averaging three or more results obtained from a 3 × 3 μm area. As shown in **Figure 7**, the average grain diameters for the TiAlN (**Figure 7a**) and TiAlN/SiNx (**Figure 7b**) films were 342 and 274 nm, respectively. In **Figure 7**, we compared the TiAlN and TiAlN/SiNx films, to show that the average grain diameter of TiAlN/SiNx was smaller than that of TiAlN. Hence, the introduction of the SiNx layer contributed to a decrease in the grain diameter [4]. The roughness of the TiAlN and TiAlN/SiNx films was determined by measuring the grain diameter and surface peak-peak height (Sy) with the AFM, where Sy is defined as the height difference between the highest and lowest peaks in the topology [4]. The

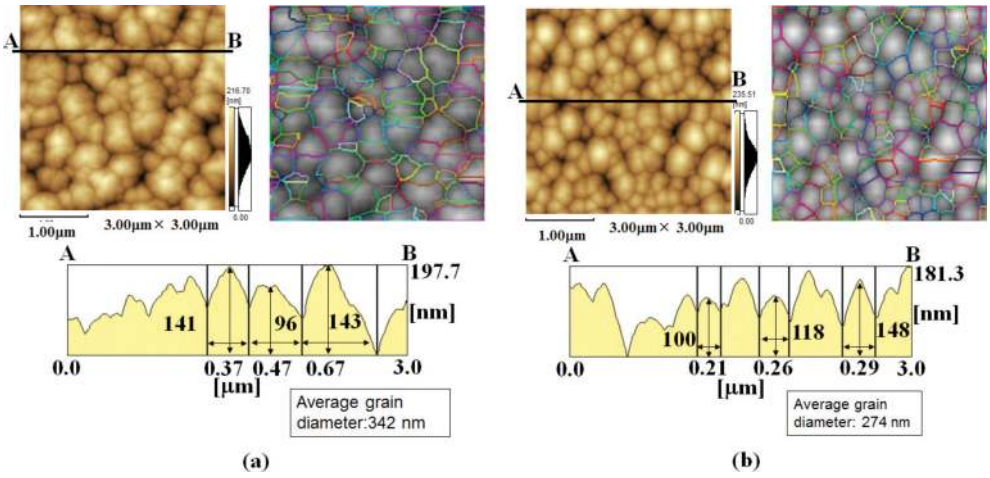

Figure 7. Surface topography map and cross-sectional image profiles of the TiAlN (a) and TiAlN/SiNx (b) films.

DFM measurement showed that the TiAlN coating had a Sy value of 211 nm. The Sy value for the TiAlN/SiNx was approximately 180 nm. Thus, the Sy of the TiAlN/SiNx coating decreased together with the grain diameter.

As shown in **Figure 8**, the average grain diameters for TiAlN + CNx (**Figure 8a**), TIAlN/CNx + TiAlN (**Figure 8b**), and TiAlN/CNx + CNx (**Figure 8c**) films were 168, 175, and 161 nm, respectively [7]. The Sy values for the TiAlN + CNx, TIAlN/CNx + TiAlN, and TiAlN/CNx + CNx films were 31.8, 46.9, and 28.2 nm, respectively. The mean grain diameters and Sy value (roughness) of the multilayer TiAlN/CNx + TiAlN and TiAlN/CNx + CNx films were smaller than that of the TiAlN film owing to the introduction of the CNx layer [7]. As a result, the average grain diameters of the TiAlN and TiAlN/CNx film decreased owing to the deposition of the CNx top layer. The TiAlN and TiAlN/CNx films consisted of an arrangement of globular grains with fine spaces and intervals, which became filled by CNx during the

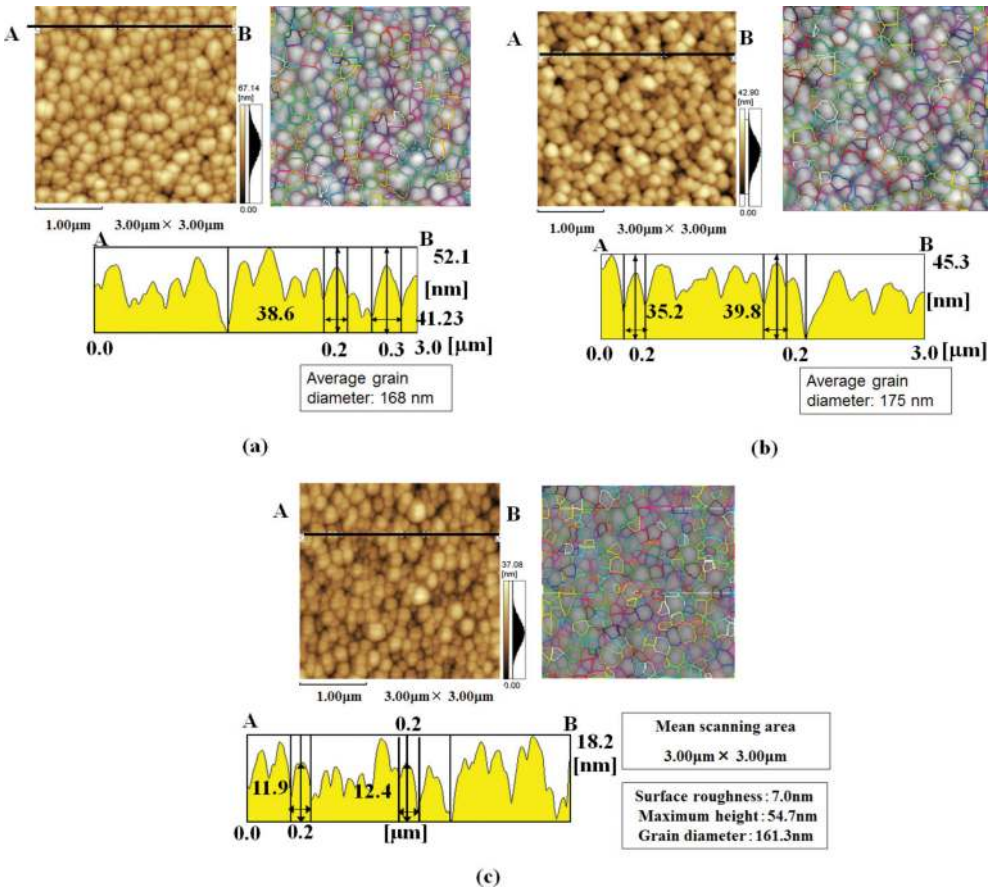

Figure 8. Surface topography map and cross-sectional image profiles of the TiAlN + CNx (a), TiAlN/CNx + TiAlN top (b) and TiAlN/CNx + CNx top films (c).

deposition of CNx as the top layer. Bonds formed between the CNx and TiAlN (or TiAlN/CNx) led to an increase in the area of boundaries [4, 7]. The morphology was related to the thickness and morphology of the top coating. The CNx top layer had a considerable effect on the surface morphology and roughness, changing the real contact area and the friction and wear behavior. Generally, the surface roughness decreased as the grain size decreased. This trend was accompanied by an improvement in the density of the morphology with a marked transition from a columnar to a fine-grained morphology [25].

The introduction of SiNx or CNx onto the TiAlN monolayer and the apparent decrease in the grain size could have contributed to the small increase of the hardness for the multilayer TiAlN/SiNx and TiAlN/CNx. The first factor that we considered was the structure parameter. When SiNx or CNx was introduced onto the TiAlN, there was a decrease in the grain size, an increase in the compressive stress level, and an improvement in the coating density accompanying the transition from a columnar to fine-grained morphology. All these factors are known to contribute to hardening of materials [25].

Factors such as residual stress, morphology, phase composition, and grain size are usually taken into account as hardening mechanisms and were considered here; however, we did not identify any major changes between the ternary and binary films that could explain the observed trend in hardness. We believed that the decrease in grain diameter might have resulted in a decrease in surface roughness, which led to the improved mechanical and tribological properties of the films [4, 7].

3.2. Evaluation of mechanical properties

The results from the characterization of the TiAlN, TiAlN/SiNx, TiAlN + CNx, TiAlN/CNx + TiAlN, and TiAlN/CNx + CNx films are summarized in **Table 1** [4, 7]. The hardness measured for TiAlN was 2590 HV. The hardness values of the multilayer TiAlN/SiNx, TiAlN/CNx + TiAlN, and TiAlN/CNx + CNx films were higher than those of the monolayer TiAlN and TiAlN + CNx films. The increase in hardness could be attributed to the introduction of a large number of TiAlN/SiNx and TiAlN/CNx interfaces in the cases of the TiAlN/SiNx and TiAlN/CNx films, respectively [4, 7]. The high hardness of the multilayer coatings is related to the role of interfaces as effective obstacles to lattice dislocation slip, which is the dominant deformation mechanism in microscale composite coatings. Owing to these interfacial and nanoscale effects, conventional lattice dislocation slip was prevented in the nanostructure

Coating	Hardness (HV0.025)	Critical Load (N)	Average grain diameter (nm)	Surface peak-peak height (Sy)
TiAlN	2590	64	342	211
TiAlN/SiNx	3200	88	274	180
TiAlN+CNx	2552	86	168	31.8
TiAlN/CNx+TiAlN	2989	127	175	46.9
TiAlN/CNx+CNx	2886	120	161	28.2

Table 1. Vickers microhardness, critical load, grain size and roughness (Sy) of monolayer and multilayer films.

coatings [4, 26, 27]. Scratch tests were conducted on the coatings and the results are shown in **Table 1**. The multilayer TiAlN/SiNx, TiAlN/CNx + TiAlN, and TiAlN/CNx + CNx films showed higher critical load values than the monolayer TiAlN and TiAlN + CNx films. These results suggest that the improved adhesion strength might be attributed to the interfaces of the multilayer preventing extension of fractures and the multilayer structure improving the wear resistance of the coating [4].

3.3. Evaluation of tribological properties

All the mono- and multilayer systems were investigated by a reciprocating SRV friction test under dry conditions, and with water and polyalphaolefin (PAO) as a lubricating film to characterize the coating frictional properties. PAO (WO-20) made by Nissan is a lubricating oil for engines and commercially available. Since PAO has characteristics such as low pour point, high viscosity index, evaporation characteristics, low traction, etc., it was used as a lubricant film in this study. The Si wafer substrates (test discs) were coated with the monolayer and multilayer systems and tested with an AISI440C ball indenter, (SUS440C, diameter: 6.0 mm). This test provided information about the cycle number dependence of the friction coefficient, and the wear behavior of the coated substrate and of its tribological counterpart. The wear volume was deduced from the wear depth created at the counterpart and was used to quantify the counterpart wear. Optical microscopy and energy dispersive X-ray spectroscopy were used to examine the wear of the coated substrate.

3.3.1. Frictional and wear properties under dry conditions

Figure 9 shows the variation of the coefficient of friction as a function of the number of sliding cycles for the investigated mono- and multilayer systems under dry conditions at room temperature. The coefficient of friction was taken as the average of four tests. Although the SiNx, TiAlNx, and TiAlN/SiNx coatings showed similar friction coefficients (1.11, 0.93, and 0.99, respectively) in frictional contact with a steel counterpart (**Figure 9a-c**), the abrasive wear of the SiNx and TiAlN coating was greater than that of the TiAlN/SiNx coating. Investigations of the wear after testing were performed with an optical microscope. Corresponding optical photomicrographs and cross-sectional images of the wear marks formed on the coatings are shown in **Figure 10**, comparing the monolayer SiNx, TiAlN, and multilayer TiAlN/SiNx films. The average cross-sectional areas of the wear tracks were measured at three or more locations after 30,000 revolutions. For the dry conditions, the wear depth of SiNx was over 29.5 μm (**Figure 10a**) and that of the TiAlN was approximately 13.6 μm (**Figure 10b**). The TiAlN/SiNx film had a wear depth of 9.9 μm (**Figure 10c**) and showed better wear resistance than that of the SiNx and TiAlN films. Although the TiAlN film showed lower friction coefficients than that of the TiAlN/SiNx film (**Figure 9a–c**), the abrasive wear of the TiAlN film was greater than that of the TiAlN/SiNx film. The wear resistance of the TiAlN/SiNx film was enhanced owing to its nanolayer microstructure and small grain size compared with that of the TiAlN film. We believe that the decrease of the grain diameter might have caused a decrease of the surface roughness, which led to the improved tribological properties of the coating. Conversely, as shown in **Figure 9c-f**, the monolayer TiAlN + CNx film showed a lower friction coefficient

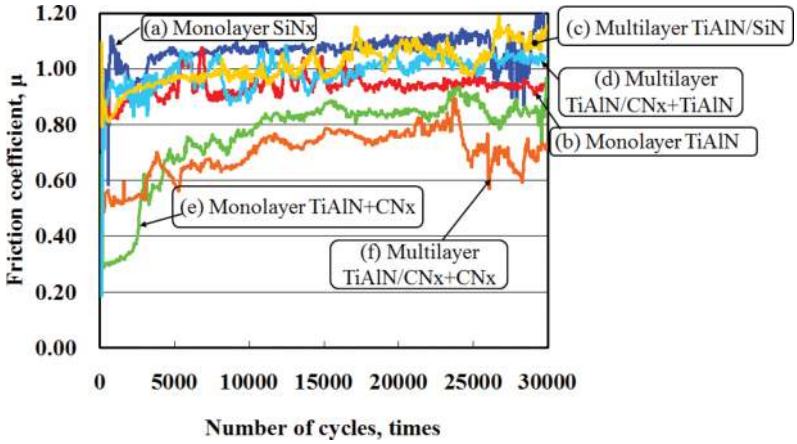

Figure 9. Friction coefficient vs. number of sliding cycles for the SRV friction test under dry conditions for: (a) SiNx, (b) TiAlN, (c) TiAlN/SiN, (d) TiAlN/CNx + TiAlN, (e) TiAlN + CNx, and (f) TiAlN/CNx + CNx coatings.

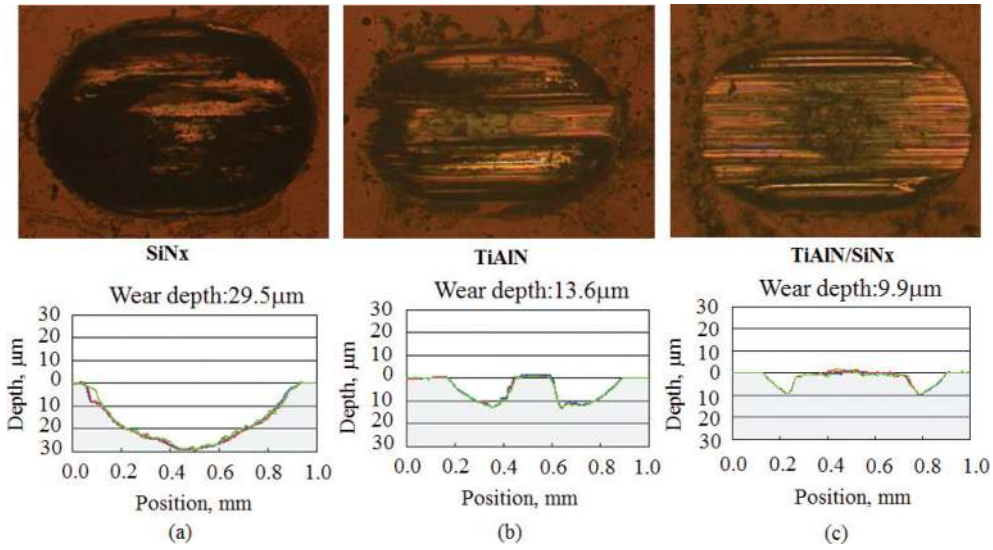

Figure 10. Wear profiles of the SiNx (a), TiAlN (b) and TiAlN/SiNx (c) coatings after SRV testing under dry conditions.

(approximately 0.71, as shown in **Figure 9e**) followed by 0.93 for the monolayer TiAlN (**Figure 9b**), 0.99 for the TiAlN/SiNx (**Figure 9c**), and 1.03 for TiAlN/CNx + TiAlN (**Figure 9d**) films. Thus, the TiAlN film with the CNx top layer had the second lowest friction coefficient of approximately 0.71. Notably, the TiAlN/CNx films with the CNx top layer had considerably lower friction coefficients than the other coatings. Furthermore, the lowest friction coefficient (approximately 0.62), which also showed a tendency to further decrease, was observed for the

multilayer TiAlN/CNx + CNx film, as shown in **Figure 9f**. Corresponding optical photomicrographs and cross-sectional images of the wear marks formed on the films are shown in **Figures 11** and **12**. The size of wear scar was calculated from the cross-sectional area of the central portion of the wear mark. The average cross-sectional areas of the wear tracks were obtained at three or more locations after 30,000 revolutions, and the size of wear scar of the

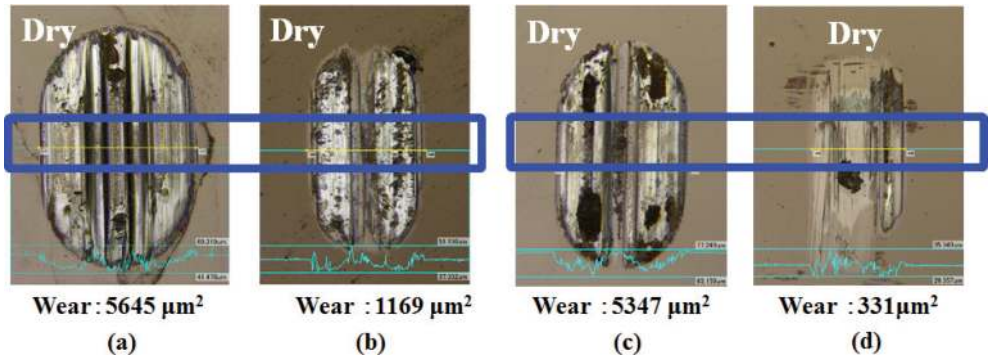

Figure 11. Wear profiles of (a) TiAlN, (b) TiAlN + CNx, (c) TiAlN/CNx + TiAlN, and (d) TiAlN/CNx + CNx coatings after SRV testing under dry conditions.

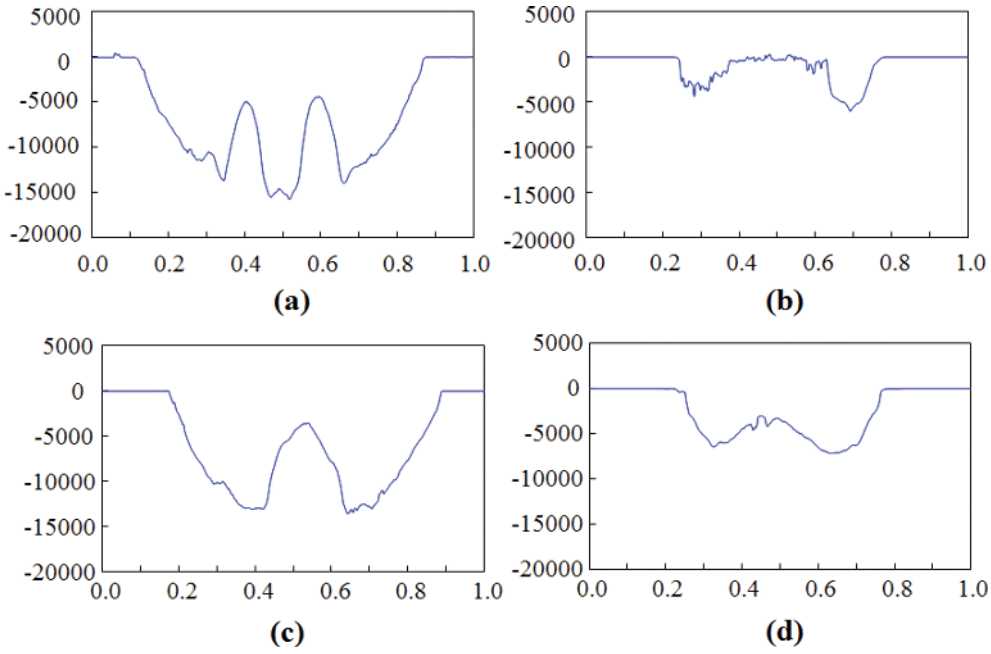

Figure 12. Cross-sectional images of wear created by SRV testing under dry conditions on (a) TiAlN, (b) TiAlN + CNx, (c) TiAlN/CNx + TiAlN, and (d) TiAlN/CNx + CNx coatings.

films were recorded after testing. The size of wear scar of the TiAlN films was greater than 5645 μm^2 (**Figures 11a** and **12a**), while that of the TiAlN/CNx + TiAlN film size was approximately 5347 μm^2 (**Figures 11c** and **12c**). However, the sizes of wear scar of the TiAlN + CNx and the TiAlN/CNx + CNx films were 1169 and 331 μm^2, as shown in **Figures 11b** and **d** and **12b** and **d**, respectively. The TiAlN/CNx + TiAlN film showed better wear resistance than the TiAlN film. The improvement in wear resistance can be attributed to the introduction of a large number of TiAlN/CNx interfaces and refinement of the multilayer microstructure. The friction coefficient and size of wear scar of the TiAlN + CNx and TiAlN/CNx + CNx films were small, such that the wear resistance values were clearly improved by the deposition of the CNx top layer because the CNx film has both wear resistance and lubricating properties [8–10].

3.3.2. Frictional and wear properties under water lubrication

The friction coefficients of the coatings were measured in the sliding system with the use of water as a lubricant. As shown in **Figure 13**, the friction coefficients of the SiNx, TiAlN, TiAlN/SiNx, TiAlN/CNx + TiAlN, TiAlN + CNx, and TiAlN/CNx + CNx films were 0.54, 0.46, 0.52, 0.45, 0.23, and 0.22 (**Figure 13a-f**, respectively). For the monolayer SiNx and TiAlN, and multilayer TiAlN/SiNx, as shown in **Figure 14**, although a large wear track (approximately 28.1 μm deep) was observed for the monolayer SiNx (**Figure 14a**), no apparent wear tracks were observed for the TiAlN (**Figure 14b**) and TiAlN/SiNx (**Figure 14c**) films under water lubrication. This result indicates that the wear resistance of the TiAlN and TiAlN/SiNx films was improved by water lubrication [4, 7].

For the TiAlN, TiAlN/CNx + TiAlN, TiAlN + CNx, and TiAlN/CNx + CNx samples, optical photographs and cross-sectional images of the wear tracks formed on the coatings are shown in **Figures 15** and **16**. The wear of the films was evaluated from the size of wear scar, as described earlier. We observed that the mean sizes of wear scar were 301, 296, 203, and 184 μm^2 for the TiAlN, TiAlN/CNx + TiAlN, TiAlN + CNx, and TiAlN/CNx + CNx films, respectively. Although

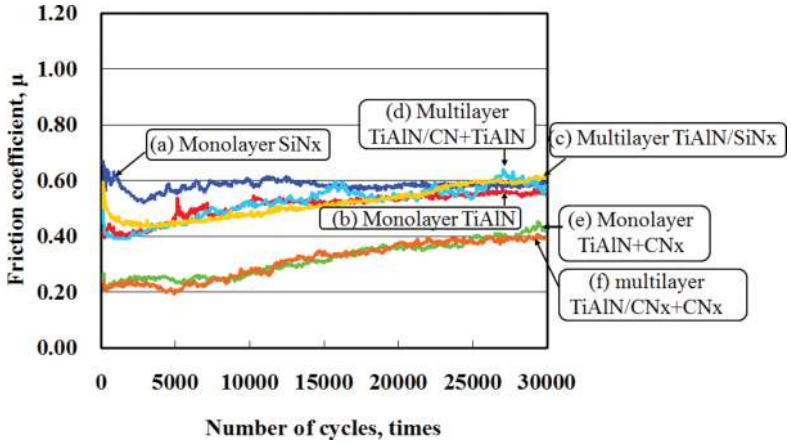

Figure 13. Friction coefficients of the coatings determined by SRV testing under water lubrication.

the TiAlN and TiAlN/CNx + TiAlN films showed similar friction coefficients, the size of wear scar of the TiAlN film is larger than that of TiAlN/CNx + TiAlN, indicating that the wear resistance of the TiAlN/CNx + TiAlN film was improved by the multilayered structure. However, the wear resistance and friction coefficients of the TiAlN + CNx and TiAlN/CNx + CNx films were considerably improved owing to the deposition of CNx [7], which has both wear resistance and lubricating properties [8–10]. This result is consistent with the reduced surface roughness and grain diameters of the films. Notably, the lowest friction and wear depths under the water lubrication conditions were obtained for the coatings with the CNx top layer, indicating that the wear resistance of the CNx layer is higher in humid air. Specifically, the lowest friction coefficients were 0.23 and 0.22 for the TiAlN + CNx and TiAlN/CNx + CNx coatings,

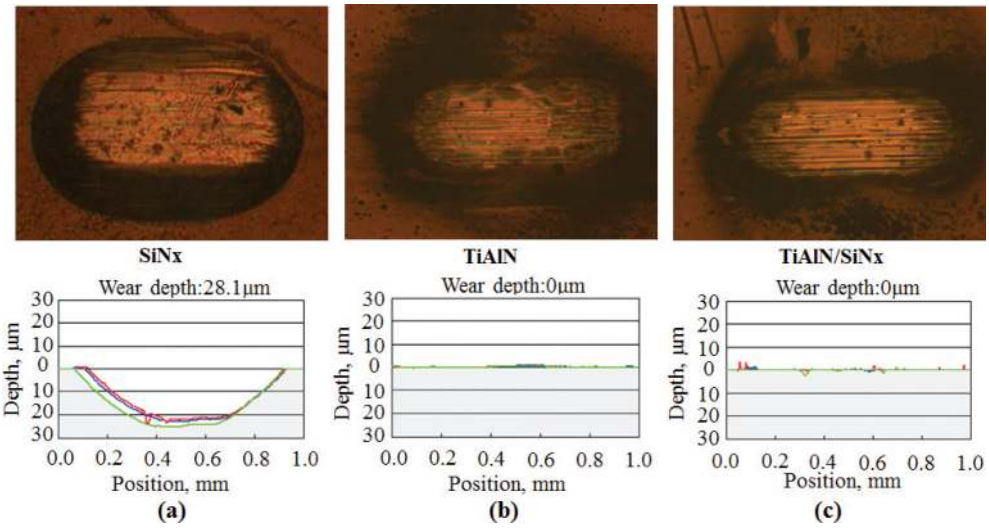

Figure 14. Wear profiles of the SiNx, TiAlN, and TiAlN/SiNx coatings after SRV testing under water lubrication.

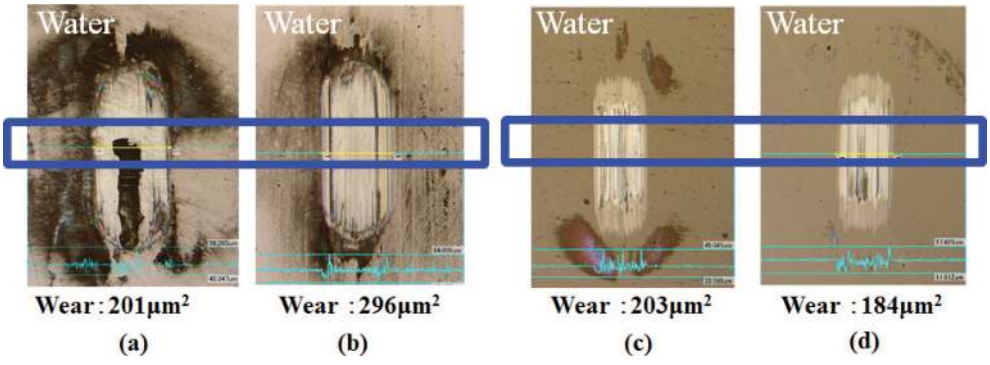

Figure 15. Wear profiles of (a) TiAlN, (b) TiAlN/CNx + TiAlN, (c) TiAlN + CNx, and (d) TiAlN/CNx + CNx coatings after SRV testing under water lubrication.

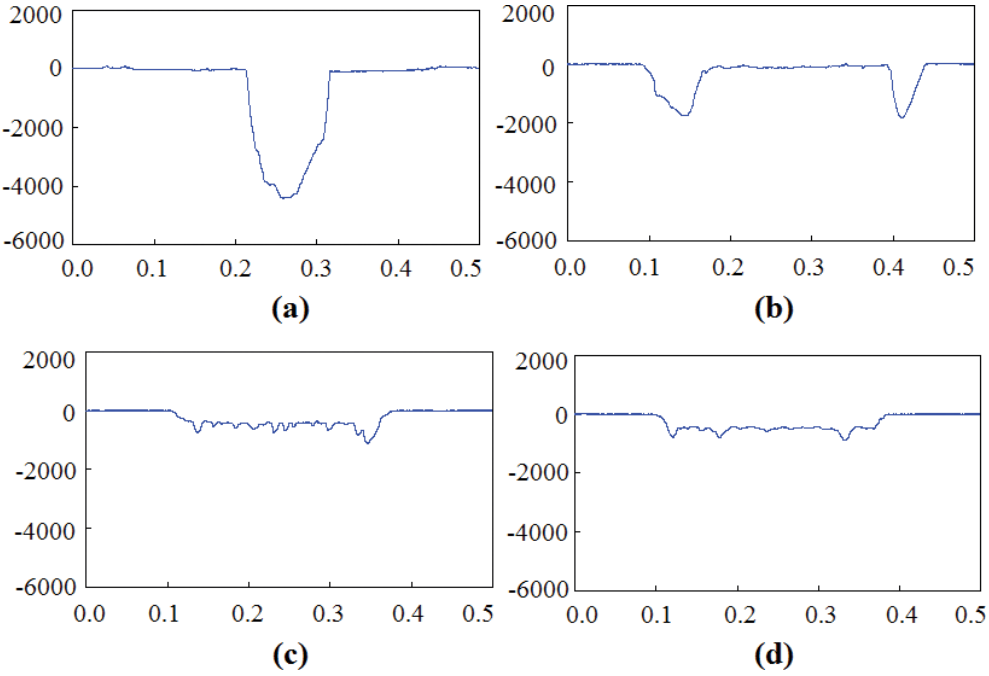

Figure 16. Cross-sectional images of wear created by SRV testing under water lubrication on the (a) TiAlN, (b) TiAlN/CNx + TiAlN, (c) TiAlN + CNx, and (d) TiAlN/CNx + CNx coatings.

values which were, respectively, 49 and 51% of the friction coefficient for the coatings without the CNx layer [7].

3.3.3. Frictional and wear properties under PAO lubrication

Figure 17 shows the variation of the coefficient of friction measured from SRV testing under PAO lubrication. The mean values of the friction coefficients for SiNx, TiAlN, TiAlN/SiNx, TiAlN/CNx + TiAlN, TiAlN + CNx, and TiAlN/CNx + CNx coatings were 0.18, 0.16, 0.19, 0.15, 0.15, and 0.14 (**Figure 17a-f**, respectively). Although the differences among the friction coefficients of the coatings was small, the TiAlN and TiAlN/CNx + TiAlN films with the CNx top layer had lower friction coefficients than those without the CNx top layer. The wear tracks formed on the coatings were observed by laser microscopy. Optical photographs and cross-sectional images of the wear tracks are shown in **Figure 18**. The size of wear scar was markedly reduced for all coatings measured by SRV testing under PAO lubrication compared with those under dry and water conditions. The sizes of wear scar were 73.0, 24.0, 14.7, and 14.3 μm^2 for the TiAlN, TiAlN + CNx, TiAlN/CNx + TiAlN, and TiAlN/CNx + CNx films. The PAO lubricant reduced the size of wear scar for the coatings with and without the CNx top layer. For the multilayer TiAlN/CNx + TiAlN, the size of wear scar of the TiAlN/CNx + TiAlN film was lower and similar to that of the TiAlN/CNx + CNx film when PAO was introduced as a

http://dx.doi.org/10.5772/intechopen.73141

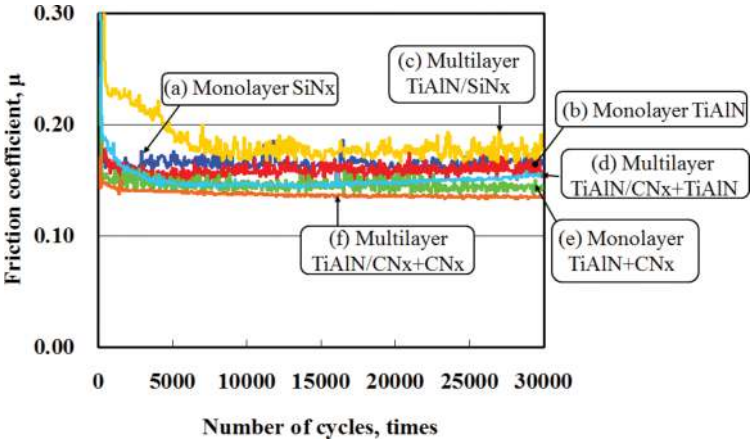

Figure 17. Average friction coefficients for monolayer and multilayer films under dry conditions and water and PAO lubrication.

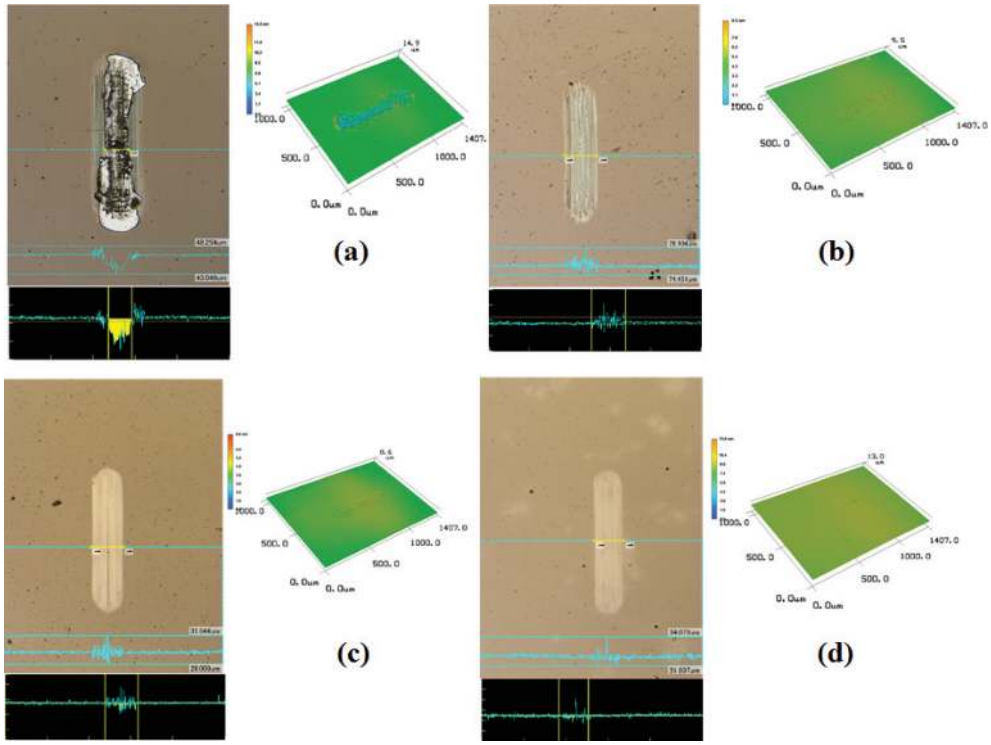

Figure 18. Images and cross-sectional of wear created by SRV testing under PAO lubrication on (a) TiAlN, (b) TiAlN/CNx + TiAlN, (c) TiAlN + CNx, and (d) TiAlN/CNx + CNx coatings.

lubricant. This result suggests that under these lubricant conditions a beneficial tribolayer forms on the wear surface, which provides a low coefficient of friction.

The friction coefficients of the films, as determined by SRV friction testing, are summarized in **Figure 19** for dry, water, and PAO conditions. The coatings with the CNx top layer showed a lower friction coefficient under dry and water conditions than the coatings without the CNx top layer. However, all the coatings showed low friction coefficients owing to the introduction of water or PAO lubricants. This result suggests that lubricants such as water and PAO can improve the tribological properties in terms of friction and wear control in, for example, cutting applications.

3.4. Performance of single layer and multilayer coatings in drilling

Single layer TiAlN, and nanoscale multilayer TiAlSiN and TiAlCrSiN coatings were prepared on cemented carbide pins and WC–Co drills by reactive magnetron sputtering deposition. The deposition conditions are detailed in previous reports [4, 7]. The tribological characteristics of the films were investigated with the use of a pin-on-disc friction test. The pin-on-disc wear test was performed at an air humidity of 50 ± 10% and a temperature of 25 ± 3°C with a pin-on-disc tribometer featuring a counterpart composed of cemented carbide [4]. The wear test was performed at a load of 2 N and a linear speed of 150 mm/s for a total sliding time of 900 s (corresponding to a sliding distance of 135 m). **Figure 20** compares the friction coefficients of the TiAlN, TiAlSiN, and TiAlCrSiN films. The TiAlCrSiN (**Figure 20c**) showed a stable and low friction coefficient in the range of 0.35–0.42; the values for TiAlN and TiAlSiN were 0.53 and 0.54, respectively (**Figure 20a** and **b**). The stable frictional properties of the TiAlCrSiN film were attributed to the nanolayer microstructure. The wear tracks formed on the films were

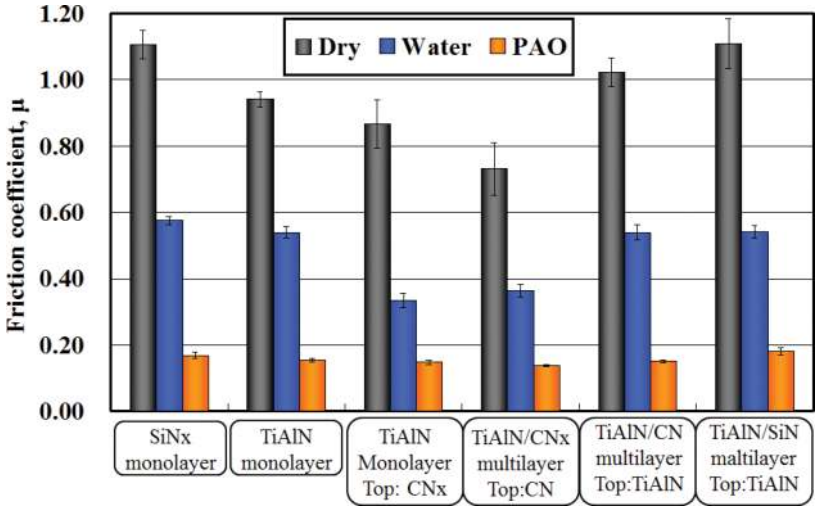

Figure 19. Average friction coefficients for monolayer and multilayer films under dry conditions and water and PAO lubrication.

observed by laser microscopy. **Figure 21** shows the profile and cross-section images of the wear tracks. The sizes of wear scar of the TiAlN (**Figure 21a**) and TiAlSiN (**Figure 21b**) coatings were 1.6×10^5 and 7.9×10^4 μm^2. The multilayer TiAlCrSiN coating (**Figure 21c**) showed a lower size of wear scar (approximately 3.6×10^4 μm^2) compared with that of the single layer TiAlN and multilayer layer TiAlSiN coatings. The wear resistance of the multilayer TiAlCrSiN coating was further improved by incorporation Cr into the TiAlSiN coating.

Friction properties and wear resistance to abrasive wear and oxidation are important characteristics for high-speed and cutting application. The lifetimes of the monolayer TiAlN, and multilayer TiAlSiN and TiAlCrSiN coated 6-mm diameter WC–Co drills (OSG Corporation, Japan) in wet (water soluble fluid) drilling of carbon steel (S50C, 50-53HRC) are shown in

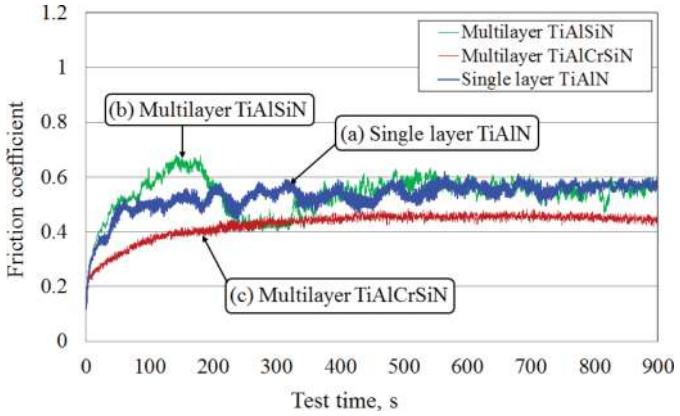

Figure 20. Friction coefficients of the coatings by pin-on-disc testing under dry conditions.

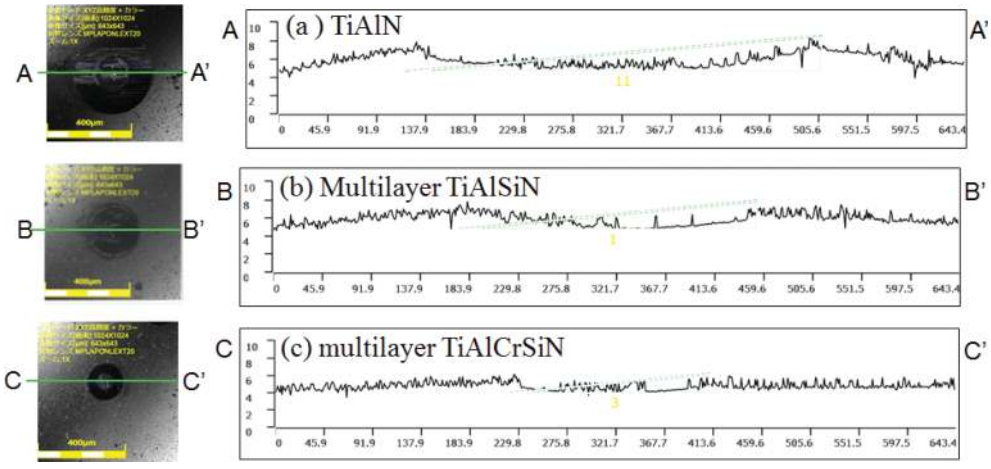

Figure 21. Wear tracks and cross-sectional images of the coatings subjected to pin-on-disc test under dry conditions.

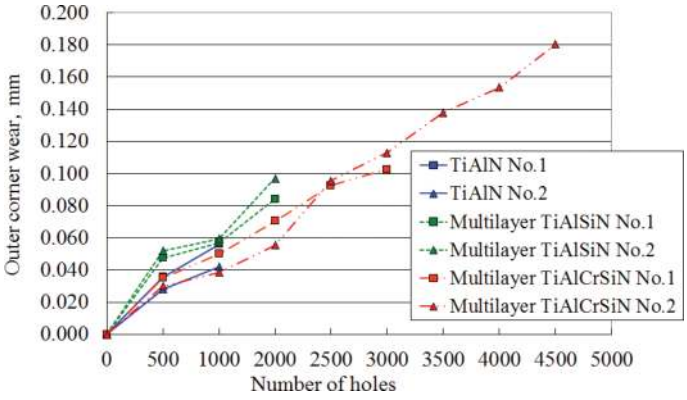

Figure 22. Outer corner wear of 6-mm diameter WC–co drills as a function of the number of holes drilled. Cutting speed: 100 m/min (5304 rpm), feed rate: 0.18 mm/rev. Workpiece: Carbon steel (S50C). Cutting fluid: Water soluble agent. Hole depth 30 mm (5×diameter).

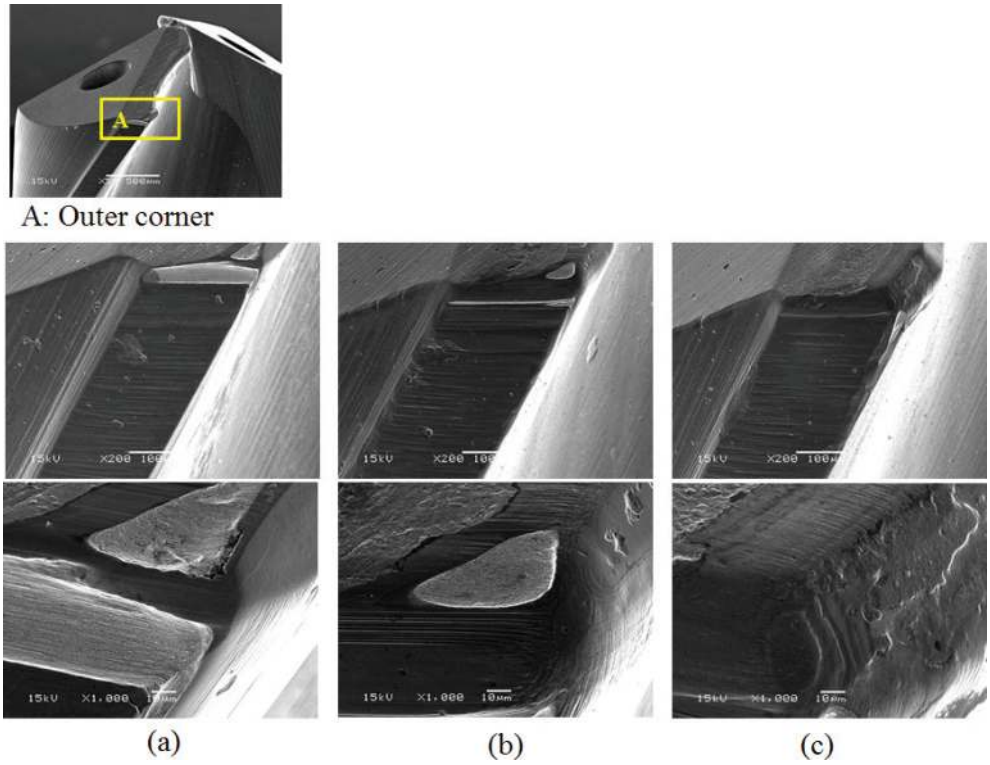

Figure 23. SEM images of the outer corner of worn areas of (a) TiAlN, (b) multilayer TiAlSiN, and (c) multilayer TiAlCrSiN coated 6 mm diameter WC–co drills after 1000-hole drilling test.

Figure 22. The performances of the multilayer TiAlSiN and TiAlCrSiN coatings were compared with that of the single layer TiAlN coating, which was used as reference. The drilling tests were performed on a drill-milling machine NH4000 (DMG MORI, Japan) at a cutting speed of 100 m/min (5304 rpm), feed rate of 0.18 mm/rev (955 mm/min), hole depth of 30 mm (5×diameter), and allowance of 0.2 mm. The lifetime of drills with the multilayer TiAlCrSiN coating was 2.01 times as long as that of the tools coated with single layer TiAlN and the multilayer TiAlSiN coatings. To investigate the differences observed in the performance of the coatings, the morphology of the outer corner flank was examined by SEM imaging. The wear patterns observed are shown in **Figure 23**. After drilling 1000 holes, the single layer TiAlN and multilayer TiAlSiN coatings showed considerable wear at the outer corner and margin of the drill bit (**Figure 23a** and **b**). Conversely, the multilayer TiAlCrSiN coated drill showed negligible wear at the outer corner and margin (**Figure 23c**). The superior drilling performance of the multilayer TiAlCrSiN coating compared with those of the single layer TiAlN and TiAlSiN coatings can be attributed to more favorable mechanical (high hardness) and tribological (low friction) properties, and wear resistance. The performance was likely enhanced by the incorporation of Cr into the multilayer TiAlSiN coating [19–22]. The low friction coefficient suggests that the decreased friction between the tool and chip in machining and a reduced tendency to stick and pick up material from the counterpart material, led to the extended service life of the cutting tool.

4. Conclusion

TiAlN monolayer, TiAlN/SiNx, TiAlN/CNx, TiAlSiN, and TiAlCrSiN multilayer coatings were deposited on WC–Co carbide tools and silicon wafer substrates by reactive magnetron sputtering. We show that the multilayer structure affects the surface morphology, microstructure, mechanical, and tribological properties.

1. The introduction of a SiNx or a CNx layer leads to the formation of hard coatings owing to suppression of the TiAlN grain growth, grain refinement, and a decrease of the surface roughness. The morphology of the coating changed from a columnar structure to a fine-grained structure when SiNx and CNx layers were formed.

2. The wear characteristics of the TiAlN/SiNx, TiAlN/CNx, TiAlSiN, and TiAlCrSiN multilayer coatings described in this study were improved compared with those of the TiAlN single layer coating. Furthermore, the tribological properties of the TiAlN and TiAlN/CNx coatings were improved owing to the deposition of CNx as the topmost layer, and the friction coefficients and size of wear scar of the coatings was decreased.

3. The wear of the TiAlN/SiNx, TiAlN + CNx, and TiAlN/CNx + CNx coatings in sliding systems was considerably reduced with the use of water as a lubricant by approximately two orders of magnitude compared with the performance under dry conditions. The wear of the coating was considerably reduced for all coatings in SRV testing under PAO lubrication conditions compared with the results obtained under dry and water conditions.

4. The tribological properties of the multilayer TiAlCrSiN-base coatings make these coatings effective at resisting wear and improved the cutting tool performance under wet conditions. The multilayer TiAlCrSiN coated drills outperformed the single layer TiAlN and multilayer TiAlSiN coated drills, which might be attributed to the multilayered structure of the TiAlCrSiN coating and to the improved tribological properties of the multilayer TiAlCrSiN coating owing to the incorporation Cr. The influence of the latter on cutting tool performance of the TiAlCrSiN coatings requires further investigation and will form part of our ongoing research into PVD coatings for dry machining in the automobile and aerospace industries.

Acknowledgements

This research was performed with the help of the graduate students at Nippon Institute of Technology.

Author details

Mei Wang[1]* and Shojiro Miyake[2]

*Address all correspondence to: mwang@osg.co.jp

1 Coating Research and Development, OSG Coating Service Co., Ltd. Aichi, Japan

2 Department of Innovative System Engineering, Nippon Institute of Technology, Saitama, Japan

References

[1] Hongmark S, Jacobson S, Larsson M. Design and evaluation of tribological coatings. Wear. 2000;**246**:20-33 https://doi.org/10.1016/S0043-1648(00)00505-6

[2] Miyake S. Tribology of carbon nitride and boron nitride nanoperiod multilayer film and its application to nanoscale processing. Thin Solid Films. 2005;**493**:160-169 https://doi.org/10.1016/j.tsf.2005.07.284

[3] Miyake S, Kaneko R. Microtribological properties and potential applications of hard, lubricating coatings. Thin Solid Films. 1992;**212**:256-261 https://doi.org/10.1016/0040-6090(92)90530-O

[4] Sakurai M, Toihara T, Wang M, Kurusaka W, Miyake S. Surface morphology and mechanical properties of nanoscale TiAlN/SiNx multilayer coating deposited by reactive magnetron

sputtering. Surface and Coating Technology. 2008;**203**:171-179 https://doi.org/10.1016/j.surfcoat.2008.08.060

[5] Nose M, Kawabata T, Khamseh S, Matsuda K, Fujii K, Ikeno S, Chiou WA. Microstructure and properties of TiAlN/a-C nanocomposite coatings prepared by reactive sputtering. Materials Transactions. 2010;**51**(2):282-287 http://doi.org/10.2320/matertrans.MC200913

[6] Kurosaka W, Shindo T, Wang M, Miyake S. Deposition and tribological properties of TiAlN/SiNx multilayer coatings. Journal of the Japan Society for precision engineering. 2012;**78–10**:905-911(in Japanese). http://doi.org/10.2493/jjspe.78.905

[7] Wang M, Toihara T, Sakurai M, Kurosaka W, Miyake S. Surface morphology and tribological properties of dc sputtered nanoscale multilayered TiAlN/CNx coatings. Tribology International. 2014;**73**:36-46 https://doi.org/10.1016/j.triboint.2014.01.008

[8] Miyake S, Watanabe S, Miyazawa H, Murakawa M, Miyamoto T, Kaneko R. Modification of nanometer scale wear of nitrogen-containing carbon films due to ion implantation. Nuclear Instruments and Methods in Physics Research. 1997;**B 122**:643-649. https://doi.org/10.1016/S0168-583X(96)00924-X

[9] Miyake S, Watanabe S, Miyazawa H, Murakawa M. Improved microscratch hardness of ion-plated carbon film by nitrogen inclusion evaluated by atomic force microscope. Applied Physics Letters. 1994;**65**(25):3206-3208 http://dx.doi.org/10.1063/1.112414

[10] Miyake S, Saito T, Wang M, Watanabe S. Tribological properties of extremely thin protective carbon nitride films deposited on magnetic discs by complex treatment. Journal of Engineering Tribology Part – J, Proceedings of the Institution of Mechanical Engineers. 2006;**220**(7):587-595. DOI: https://doi.org/10.1243/13506501JET124

[11] Wang M, Miyake S, Saito T. Nanoindentation and nanowear of extremely thin protective layers of C-N and B-C-N. Tribology International. 2005;**38**(6–7):657-664 https://doi.org/10.1016/j.triboint.2005.03.001

[12] Miyake S, Hashizume T, Kurosaka W, Sakurai M, Wang M. Deposition and tribology of carbon and boron nitride nanoperiod multilayer solid lubricating films. Surface and Coating Technology. 2007;**202**(4–7):1023-1028 https://doi.org/10.1016/j.surfcoat.2007.07.079

[13] Liu CS, Zheng ZY, DW W, Ye MS, Gao P, Peng YG, Fan XJ. Sliding friction and wear properties of CNx /TiN composite films. Tribology International. 2004;**37**(9):721-725 https://doi.org/10.1016/j.triboint.2004.03.001

[14] Zheng XH, Tu JP, Song RG. Microstructure and tribological performance of CN(x)–TiN(x) composite films prepared by pulsed laser. Material Design. 2010;**31**:1716-1719. https://doi.org/10.1016/j.matdes.2009.01.043

[15] Wang TS, DL Y, Tian YJ, Xiao FR, He JL, Li DC, Wang WK, Li L. Cubic-C3N4 nanoparticles synthesized in CNx/TiNx multilayer films. Chemical Physics Letters. 2001;**334**(1–3):7-11 https://doi.org/10.1016/S0009-2614(00)01251-3

[16] Liu ZJ, Vyas A, YH L, Shen YG. Structural properties of sputter-deposited CNx/TiN multilayer films. Thin Solid Films. 2005;**479**:31-37 https://doi.org/10.1016/j.tsf.2004.11.106

[17] Cao M, Li DJ, Deng XY, Sun X. Synthesis of nanoscale CNx/TiAlN multilayered coatings by ion-beam-assisted deposition. Journal of Vacuum Science and Technology. 2008;**A 26–5**:1314-1318. http://dx.doi.org/10.1116/1.2956627

[18] Riedo E, Chevrier J, Comin F, Brune H. Nanotribology of carbon based thin films: The influence of film structure and surface morphology. Surface Science. 2001;**477**:25-34 https://doi.org/10.1016/S0039-6028(01)00701-4

[19] Derflinger VH, Schutze A, Ante M. Mechanical and structure properties of various alloyed TiAlN-based hard coatings. Surface and Coatings Technology. 2006;**200**:4693-4700 https://doi.org/10.1016/j.surfcoat.2005.02.065

[20] Kao CM, Lee JW, Chen HW, Chan YC, Duh JG, Chen SP. Microstructures and mechanical properties evaluation of TiAlN/CrSiN multilayered thin films with different bilayer periods. Surface Coatings and Tehnology. 2010;**205**:1438-1443 https://doi.org/10.1016/j.surfcoat.2010.07.107

[21] Donohue LA, Smith IJ, Munz W-D, Petrov I, Greene JE. Microstructure and oxidation-resistance of Ti1-x-y-zAlxCryYzN layers grown by combined steered-arc/unbalance-magnetron-sputter deposition. Surface and Coating Technology. 1997;**94-95**:226-231

[22] Simth IJ, Munz W-D, Donohue LA, Petrov I, Greene JE. Improved Ti1-xAlxN PVD coatings for dry high speed cutting operations. Surface Coatings and Technology. 1998;**14-1**:37-41. http://dx.doi.org/10.1179/sur.1998.14.1.37

[23] Watanabe S, Noshiro J, Miyake S. Tribological characteristics of WS2/MoS2 solid lubricating multilayer films. Surface and Coating Technology. 2004;**183**:347-351 https://doi.org/10.1016/j.surfcoat.2003.09.063

[24] Thornton JA, Hoffman DW. Stress-related effects in thin films. Thin Solid Films. 1989;**171**:5-31 https://doi.org/10.1016/0040-6090(89)90030-8

[25] Nanostructured Coatings, Edited by, Part of the Nanostructure Science and Technology book series (NST). New York, NY: Springer. Print ISBN 978-0-387-25642-9. pp. 253-270 https://doi.org/10.1007/978-0-387-48756-4

[26] Veprek S, Reiprich S. A concept for the design of novel superhard coatings. Thin Solid Films. 1995;**268**:64-71 https://doi.org/10.1016/0040-6090(95)06695-0

[27] Niederhofer A, Bolom T, Nesladek P, Moto K, Eggs C, Patil DS, Veprek S. The role of percolation threshold for the control of the hardness and thermal stability of super- and ultrahard nanocomposites. Surface and Coating Technology. 2001;**183**:146-147 https://doi.org/10.1016/S0257-8972(01)01469-4